Antimicrobial chitosan nanodroplets: New insights for ultrasound-mediated adjuvant treatment of skin infection [*G. Banche and M. Prato contributed equally to this work; ** M. Prato is the corresponding author]

UNIVERSITÀ DEGLI STUDI DI TORINO

Antimicrobial chitosan nanodroplets: new insights for ultrasound-mediated adjuvant treatment of skin infection.

Giuliana Banche[1,#], Mauro Prato[1*,2,#], Chiara Magnetto[3], Valeria Allizond[1], Giuliana Giribaldi[4], Monica Argenziano[5], Amina Khadjavi[2], Giulia Rossana Gulino[4], Nicole Finesso[4], Narcisa Mandras[1], Vivian Tullio[1], Roberta Cavalli[5], Caterina Guiot[2] & Anna Maria Cuffini[1]

[1] *Dipartimento di Scienze della Sanità Pubblica e Pediatriche, Università di Torino, Torino, Italy*

[2] *Dipartimento di Neuroscienze, Università di Torino, Torino, Italy*

[3] *Istituto Nazionale di Ricerca Metrologica (INRIM), Torino, Italy*

[4] *Dipartimento di Oncologia, Università di Torino, Torino, Italy*

[5] *Dipartimento di Scienza e Tecnologia del Farmaco, Università di Torino, Torino, Italy*

 # These authors equally contributed to the work

* Author for correspondence. Tel.: +39-011-670-8198; Fax: +39-011-670-8174; E-mail: mauro.prato@unito.it

Abstract

Chronic wounds, characterized by hypoxia, inflammation, and impaired tissue remodeling, are often worsened by bacterial/fungal infections. Intriguingly, chitosan-shelled/decafluoropentane-cored oxygen-loaded nanodroplets (OLNs) have proven effective in delivering oxygen to hypoxic tissues. Here, nanodroplet antimicrobial properties against methicillin-resistant *Staphylococcus aureus* (MRSA) or *Candida albicans*, toxicity on human keratinocytes (HaCaT), and ultrasound (US)-triggered transdermal delivery were investigated. OLNs and oxygen-free nanodroplets (OFNs) displayed short- or long-term cytostatic activity against methicillin-resistant *Staphylococcus aureus* or *Candida albicans*, respectively. OLNs were not toxic to keratinocytes, whereas OFNs slightly affected cell viability. Complementary US treatment promoted OLN transdermal delivery. As such, US-activated chitosan-shelled OLNs appear as promising, nonconventional and innovative tools for adjuvant treatment of infected chronic wounds.

Key words

Chitosan; oxygen; nanodroplet; methicillin-resistant *Staphylococcus aureus* (MRSA); *Candida albicans*; skin.

Abbreviations used in this paper

OLN, oxygen-loaded nanodroplet; OFN, oxygen-free nanodroplet; MRSA, methicillin-resistant *Staphylococcus aureus*; US, ultrasound; DFP, 2H,3H-decafluoropentane; PFP, perfluoropentane; PBS, phosphate-buffered saline; UV, ultraviolet; MW, molecular weight; CFU, colony-forming unit; LDH, lactate dehydrogenase; MTT, 3-(4,5-dimethylthiazol-2-yl)-2,5-diphenyltetrazolium bromide; ANOVA, Analysis of Variance.

Chronic wounds including ulcers, bedsores, burns, and diabetes-associated vasculopathies represent a global issue costing millions of dollars per year in developed countries [1]. Beyond delayed healing processes due to insufficient oxygen supply to tissues, persistent inflammation, and impaired balances between proteinases and their inhibitors involved in tissue remodelling, chronic wounds are often worsened by microbial complications such as local or overt infection, and spread of multiresistant germs [2]. In particular, methicillin-resistant *Staphylococcus aureus* (MRSA) and *Candida albicans* are two frequent pathogens involved in chronic wounds in patients with diabetes or in immunocompromised subjects [3-4]. Therefore, wound management is a major challenge requiring new solutions against microorganisms and their biofilms [5].

Antibiotic and/or antimycotic therapies are generally considered the gold standard to treat overt infections. However, the emergency of microbial drug resistance [5] along with the limited efficacy of transdermal drug delivery due to low permeability of the stratum corneum [6] are driving the attention towards new approaches, especially for patients displaying high risk of infection. Nanotechnology has become a major area of interest as a consequence of its many unique characteristics. Indeed, nanoparticles feature several physico-chemical properties such as high surface-to-volume ratio and small size that allow to pass through the interendothelial gaps of fenestrated capillaries [7-8]. Upon direct interaction of nanoparticles with cell membrane/wall proteins and key enzymes, microbial growth can be inhibited and cell death promoted through other mechanisms than antibiotics. Intriguingly, nanoparticle physico-chemical characteristics can also be manipulated to promote these molecular interactions and improve their action [7-8].

The emerging evidence on antimicrobial properties of several natural substances such as chitosan and silver compounds [9] combined with the achieved progresses of green nanotechnology [10] have paved the way to develop nonconventional and innovative therapies for infected chronic wounds. Furthermore, a major role for ultrasound (US) to promote transdermal drug delivery through sonophoresis-dependent mechanisms has been recently proposed [11]. US was also shown

to be pivotal in inducing gas release from perfluoropentane (PFP)-cored nanobubbles as a consequence of cavitation events [12-13].

In this context, we recently developed a new platform of US-responsive oxygen nanocarriers, named oxygen-loaded nanodroplets (OLNs). US-activated OLNs, constituted of biocompatible and biodegradable polysaccharidic shells (chitosan or dextran) and nontoxic oxygen-storing fluorocarbon (2H,3H-decafluoropentane, DFP) inner cores, are effectively able to deliver oxygen to cutaneous tissues both *in vitro* and *in vivo* [14-15]. Given chitosan antimicrobial and immunological properties, in the present work we investigated whether OLNs might be considered as useful tools to target infection in chronic wounds. As such, chitosan OLNs were tested for their antimicrobial properties against MRSA and *C. albicans*, as well as for cytotoxicity on human keratinocytes. Furthermore, the role of US in eliciting chitosan OLN delivery throughout skin tissues was explored.

Materials & Methods

- Materials

Unless otherwise stated, all materials were from Sigma-Aldrich (St Louis, MO). Ethanol (96%) was from Carlo Erba (Milan, Italy); Epikuron 200® (soya phosphatidylcholine 95%) was from Degussa (Hamburg, Germany); Trypticase Soy Broth and Agar (TSB, TSA) and Sabouraud dextrose (SAB) broth and agar were from Oxoid SpA (Garbagnate Milanese, Italy); cryovials were from Microbank, BioMérieux (Rome, Italy); cell culture Dulbecco's modified Eagle's medium (DMEM) was from Invitrogen (Carlsbad, CA); Ultra-Turrax SG215 homogenizer was from IKA (Staufen, Germany); Stratalinker® UV Crosslinker 1800 was from Stratagene (La Jolla, CA); Delsa Nano C analyzer was from Beckman Coulter (Brea, CA); Synergy HT microplate reader was from Bio-Tek Instruments (Winooski, VT); Stereoscan 410 for Scansion Electron Microscopy (SEM) and Leitz instrument for fluorescent microscopy was from Leica Microsystems (Wetzlar, Germany); Ubbelohde capillary viscosimeter was from Schott Gerate (Munich, Germany); RF-550 spectrofluorimeter was from Shimadzu (Columbia, MD).

- Nanodroplet preparation and characterization

OLNs and oxygen-free nanodroplets (OFNs) were prepared as previously described [14]. Briefly, 1.5 ml DFP, 0.5 ml polyvinylpyrrolidone and 1,8 ml Epikuron® 200 (solved in 1% w/v ethanol and 0.3 % w/v palmitic acid solution) were homogenized in 30 ml phosphate-buffered saline (PBS) solution (pH 7.4) for 2 min at 24000 rpm by using Ultra-Turrax SG215 homogeniser. For OLNs, the solution was saturated with O_2 for 2 min. Finally, 1.5 ml solution of chitosan [medium molecular weight (MW): 190-310 kDa; deacetylation degree: 75-85%] was added drop-wise whilst the mixture was homogenised at 13000 rpm for 2 min. Immediately after manufacturing, nanodroplets were sterilized through ultraviolet (UV)-C ray exposure for 20 min using Stratalinker® UV Crosslinker 1800. Thereafter, OLN and OFN formulations were characterized for morphology, average diameters, size distribution, zeta potential, oxygen content, viscosity, and stability. Morphology was observed through SEM analysis: briefly, a drop from the diluted nanodroplet aqueous

suspension was placed on Leica Stereoscan 410 microscope stub, and was subsequently metalized with graphite. Average diameters, size distribution, and zeta potential were investigated by light scattering employing a Delsa Nano C analyzer as previously described [14-15]. Oxygen content was measured through a well-established chemical assay [14-15]: briefly, nanodroplets were evaluated by adding known amounts of sodium sulfite and measuring generated sodium sulfate, according to the reaction:

$$Na_2SO_3 + O_2 \rightarrow Na_2SO_4$$

The viscosity of nanodroplet formulations was determined through a Ubbelohde capillary viscosimeter. Furthermore, the stability of nanodroplet formulations was evaluated over time by checking all these parameters at 4°C, 25°C or 37°C up to 6 months.

- Bacteria, yeasts, and human cells

MRSA and *C. albicans* were cultured at 37°C on TSA or SAB agar, respectively. Both strains were isolated from human ulcerated wounds. Young colonies (18–24 h) were picked up to approximately 3–4 McFarland standard and inoculated into cryovials containing both cryopreservative fluid and porous beads to allow microorganisms to adhere [16]. After inoculation, cryovials were kept at –80°C for extended storage. Lastly, HaCaT cell line, immortalised from a 62-year old Caucasian male donor [17], was used as source of human keratinocytes. Cells were grown as monolayers in DMEM supplemented with 10% fetal bovine serum, 100 U/ml penicillin, 100 μg/ml streptomycin, and 2 mM L-glutamine in a humidified CO_2/air-incubator at 37°C.

- Microbiological assays

MRSA or *C. albicans* [10^4 Colony Forming Units (CFU)/ml] were incubated in TSB or SAB broth with/without 10% v/v OLN or OFN PBS suspensions in sterile sampling tubes for 2, 3, 4, and 24 h at 37°C. Alternatively, 0.5% Triton X-100 was added to cells as an effective cytotoxic agent (positive control). At each incubation

time, serial 10-fold dilutions from each sample were prepared in 0.9% NaCl saline solution and 100 µl of each dilution was spread on TSA or SAB agar medium to determine the number of CFU/ml.

- Cytotoxicity assay

The potential cytotoxic effects of nanodroplets were measured as the release of lactate dehydrogenase (LDH) [18] from HaCaT cells into the extracellular medium. Cells (10^6/2 ml) were incubated in DMEM with/without 10% v/v OLN or OFN PBS suspensions in normoxic (20% O_2) or hypoxic (1% O_2) conditions for 24 h. Alternatively, 0.5% Triton X-100 was added to cells as an effective cytotoxic agent (positive control). After collection, cell supernatants and lysates were diluted with 82.3 mM triethanolamine (pH 7.6) and supplemented with 0.5 mM sodium pyruvate and 0.25 mM NADH (300 µL as a final volume). The reaction was monitored by measuring the absorbance at 340 nm (37 °C) with Synergy HT microplate reader. After determining the intracellular and extracellular LDH activities, expressed as µmol of oxidized NADH/min/well, cytotoxicity was eventually calculated as the net ratio between extracellular and total (intracellular + extracellular) LDH activities [18].

- Cell viability assay

Cell viability was evaluated using 3-(4,5-dimethylthiazol-2-yl)-2,5-diphenyltetrazolium bromide (MTT) assay [14]. Cells (10^6/2 ml) were incubated in DMEM with/without 10% v/v OLN or OFN PBS suspensions in normoxic (20% O_2) or hypoxic (1% O_2) conditions for 24 h. Alternatively, 0.5% Triton X-100 was added to cells as an effective cytotoxic agent (positive control). Thereafter, DMEM was discarded and 5 mg/mL MTT in 20 µL PBS was added to cells for 3 h at 37 °C. After plate centrifugation and cell supernatant discarding, the dark blue formazan crystals were dissolved using 100 µL of lysis buffer containing 20% (w/v) sodium dodecyl sulfate, 40% N,N-dimethylformamide (pH 4.7 in 80% acetic acid). The plates were then read on Synergy HT microplate reader at a test wavelength of 550 nm and at a reference wavelength of 650 nm.

- Sonophoresis assay

High frequency US ability to trigger OLN trespassing of skin layers and subsequent oxygen release was tested *in vitro* by using a home-made apparatus consisting of two sealed cylindrical chambers (donor and recipient, respectively) separated by a layer of pig ear skin [14-15]. Skin slices were isolated with a dermatome from outer side of pig ears, obtained from a local slaughterhouse, and then were frozen at −18 °C. Before the experiments the skin was equilibrated in saline solution (NaCl 0.9% w/w), added with sodium azide (0.01%) to preserve the skin, at 25 °C for 30 min. Then, after washings with saline solution, the skin layer was inserted between the two compartments of the modified Franz cell, with the *stratum corneum* side facing towards the donor chamber. The donor chamber (filled with OLNs) was connected to an US-transducer (f = 2.5 MHz; P = 5 W), which was alternatively switched on and off at regular time intervals of 5 min for 135 min. Thereafter, the passage of OLNs from the donor to the recipient chamber was visualized by optical microscopy using a Leitz instrument. Chitosan amounts were also quantified as described in paragraph 2.9.

- Quantitative determination of fluorescent chitosan

The quantitative determination of chitosan was carried out through a fluorimetric assay [19]. The external standard method was used. To obtain the calibration curve a series of chitosan standard solutions at pH 5.0 were prepared in the concentration range between 0.5 - 10 μg/ml. Then, chitosan standard solutions were added to fluorescamine solubilized in dimethyl sulfoxide (2 mg/ml) and incubated for 30 minutes in the dark. After dilution with a phosphate buffer 0,02 M at pH 8.5, the fluorescence of solutions was detected. To determine the chitosan amount present in the donor and recipient phases, 500 μl of each sample were added to 500 μl of fluorescamine solution in dimethyl sulfoxide (2 mg/ml). After 30 minutes of incubation in the dark, the samples were diluted using phosphate buffer 0,02 M at pH 8.5 and analyzed by a spectrofluorimeter (λ_{exc} = 384 nm and λ_{em} = 489 nm).

- Statistical analysis

Three independent experiments were performed for every investigational study. Numerical data are shown as means ± SEM for inferential results or as means ± SD for descriptive results. Imaging data are shown as representative pictures. All data were analyzed by a one-way Analysis of Variance (ANOVA) followed by Tukey's post-hoc test (software: SPSS 16.0 for Windows, SPSS Inc., Chicago, IL).

Results

- Characterization of chitosan nanodroplets

After manufacturing, OLN and OFN preparations were characterized for: morphology, by SEM; size distribution, polydispersity index, and zeta potential, by dynamic light scattering; oxygen content through a chemical assay; and viscosity through a rheometer. Results are shown in **Figure 1** and **Tables 1-2**. Both OLNs and OFNs displayed spherical shapes. All sizes were in the nanometer range, with average diameters ranging from ~300 nm (OFNs) to ~700 nm (OLNs). Polidispersity indexes were 0.10 and 0.12 for OLN and OFN preparations, respectively. Zeta potentials ranged from ~ + 34 mV (OFNs) to ~ + 35 mV (OLNs). OLNs also displayed a good oxygen-storing capacity (~ 0.45 mg/ml of oxygen). Both chitosan-shelled OLN and OFN formulations displayed similar viscosity (~4.6 cP) either before or after UV irradiation. Such a value was comparable to that obtained from a solution containing free chitosan (~4.6 cP), suggesting that UV sterilization did not alter the degree of chitosan deacetylation in nanodroplet formulations [20]. OLN and OFN preparations also proved to be physically stable over time, as confirmed by long-term (up to six months) checking of these parameters.

- Chitosan nanodroplets are cytostatic against MRSA and *C. albicans*

Antimicrobial properties of chitosan nanodroplets were tested both on bacterial and fungal strains. Either MRSA or *C. albicans* (10^4 CFU/ml) were incubated alone (negative controls), in the presence of 10% v/v OLN or OFN PBS suspensions, or with 0.5% Triton X-100 (positive controls) in sterile conditions at 37°C and their growth was monitored for 2, 3, 4, and 24 h. As shown in **Figure 2**, both OLNs and OFNs significantly inhibited either bacterial or fungal growth at earlier time-points, whereas at the end of the observational period they displayed cytostatic effects only against *C. albicans*. No significant differences were observed between OLN and OFN treatments. As expected, 0.5% Triton X-100 was 100% cytotoxic (not shown). Of

note, additional US administration (f = 1 MHz; P = 5 W; t = 10 min) did not significantly alter OLN and OFN effects on microbial counts (not shown).

- Oxygen loading prevents chitosan nanodroplets from toxicity to human keratinocytes

The potential nanodroplet toxicity on human skin cells was assessed by testing *in vitro* cultured HaCaT keratinocytes. Cells were incubated for 24 h alone (negative controls), with 10% v/v OLN or OFN PBS suspensions, or with 0.5% Triton X-100 (positive controls) in normoxic (20% O_2) or hypoxic (1% O_2) conditions. Thereafter, nanodroplet toxicity was analyzed by LDH assay, and cell viability by MTT assay. As shown in **Figure 3**, OFNs displayed an average 15% toxicity, compromising keratinocyte viability either under normoxic or hypoxic conditions. On the contrary, OLNs did not show toxic effects and did not significantly affect HaCaT cell viability, both in normoxia and hypoxia. As expected, 0.5% Triton X-100 was 100% cytotoxic (not shown).

- US promotes transdermal delivery of chitosan OLNs

To evaluate US efficacy in inducing OLN transdermal delivery, a sonophoresis assay constituted by two chambers separated by a pig skin layer was employed. As shown in **Figure 4**, OLN presence in both chambers was evaluated before and 135 min after US treatment by optical microscopy. US effectively induced sonophoresis and promoted OLN trespassing of the pig skin layer. These observations were further confirmed by quantifying the levels of chitosan in both chambers before and after US treatment through a fluorimetric assay (**Table 3**). As an average, 15% of total chitosan OLNs was found in the recipient chamber at the end of the experiment.

Discussion

DFP-based nanodroplets are a new platform of biocompatible and therapeutically multi-faceted gas nanocarriers recently developed by our group [14-15]. Intriguingly, chitosan-shelled OLNs, characterized by spherical morphology, ~700 nm diameters, cationic surfaces, and good oxygen-carrying capacity, have been shown to effectively release oxygen to cutaneous tissues upon complementary US administration both *in vitro* and *in vivo* [14]. Nanodroplet formulations can be sterilized by UV-C rays. UV irradiation does not induce singlet oxygen generation [14] and does not alter their viscosity. Since the degree of chitosan deacetylation directly correlates with viscosity [20], it should be assumed that no alterations in the degree of deacetylation of the nanodroplet shell polysaccharide occur upon UV sterilization.

In this work chitosan-shelled nanodroplets (either with or without oxygen) were challenged for their antimicrobial properties in order to assess whether they might be considered as good candidate tools for topical treatment of infected wounds. Interestingly, both OLNs and OFNs showed significant cytostatic activity against MRSA and *C. albicans*, with the antifungal activity being more sustained over time than the antibacterial. Antimicrobial activity is a likely consequence of the presence of chitosan in the shell of nanodroplets and appears to be independent from the presence or absence of oxygen in the inner core. Indeed, in recent years consistent evidence has supported the employment of this natural polysaccharide as an antimicrobial, anti-inflammatory and wound healing accelerant. Chitosan is a positively charged, partially deacetylated form of chitin, a natural substance found abundantly in the exoskeletons of insects and the shells of crustaceans [21]. The repeating units of chitosan are ϐ(1-4)-linked glucosamines, thus it contains a large number of hydroxyl- and amino-groups providing several possibilities for derivatisation or grafting of desirable bioactive groups [22]. Chitosan amino groups display pKa values of ~6.5. As such, depending on the degree of deacetylation of the polysaccharide, they can be protonated in weakly acidic conditions, thus allowing chitosan to interact with negatively-charged microbial cell walls or membranes, decreasing

osmotic stability and promoting membrane disruption and leakage of intracellular elements [23]. After being uptaken by bacteria and fungi , chitosan can bind microbial DNA, inhibiting mRNA and protein synthesis [7, 24]. According to literature [23], chitosan MW and deacetylation degree are inversely proportional to its antimicrobial activity. Note that the type of chitosan chosen for nanodroplet manufacturing is characterized by a medium MW (190-310 kDa) and a low deacetylation degree (75-85%), thus justifying the results obtained from the present study.

Furthermore, chitosan displays several immunological functions, as it is able to inhibit the expression and release of pro-inflammatory cytokines, promote fibroblast recruitment and tissue granulation, and induce the production of type III collagen [25]. Unfortunately, chitosan clinical use has been limited by its poor solubility at physiologic pH [26]. Interestingly, it has been proposed that charged nanoparticles are exquisitely suitable for topical treatment, since surface charges enhance nanoparticle interaction with the skin and improve their therapeutic effect on inflamed cutaneous tissues. In particular, cationic nanoparticles are generally recommended for topical treatment due to the anionic nature of the skin [27].

In this context, the cationic nanocarrier platform employed here should hopefully overcome chitosan limitations without losing its potent antimicrobial activity; even more so, DFP-based nanodroplets may be employed as a delivery system to incorporate additional therapeutics. Extensive toxicity and absorption, distribution, and excretion data exist on neat and emulsified fluorocarbons such as DFP, as a result of intensive research and development efforts on their use in blood substitutes, liquid ventilation, and drug delivery. These molecules are extremely stable and biologically inert, can be manufactured at very high purity, and are rapidly excreted into the expired air in a nonmetabolized form after injection into the bloodstream [28].

The potential toxicity of nanodroplets was investigated by testing *in vitro* cultures of human HaCaT keratinocytes immortalized from a 62-year old donor [17]. This cell line was chosen because hypoxia effects on wound repair-associated matrix metalloproteinases are strongly influenced by donor's age, and hypoxia-associated skin pathologies such as chronic wounds are more frequent in the elderly [29]. According to the

results from LDH and MTT analyses, OFN suspensions were slightly toxic to HaCaT keratinocytes at the texted doses, both in normoxic and hypoxic conditions. This might be a consequence of the type of chitosan chosen for nanodroplet manufacturing (medium MW chitosan), as it has been reported that chitosan molecules exhibit a MW-dependent negative effect on HaCaT cell viability and proliferation *in vitro* [30]. On the contrary, OLNs did not display any significant cytotoxicity, apparently suggesting a protective role for oxygen on keratinocyte viability. However, it should be also taken in account that OLN diameters are almost double than those of OFNs. Therefore, the lack of toxicity of OLNs with respect to OFNs may also be a consequence of such a difference in their sizes. Physico-chemical properties of nanoparticles strongly modulate the cellular uptake efficiency. After interacting with the cellular membrane, nanoparticles are generally engulfed in membrane invaginations and internalized by cells through time-, concentration- and energy-dependent pinocytic processes (macropinocytosis, clathrin-mediated endocytosis, caveolae-mediated endocytosis and mechanisms independent of clathrin and caveolin) [31-32]. In turn, these processes can activate different intracellular signaling pathways, thus paving the way for alternative cellular fates, from proliferation to apoptosis, from survival to death [33-35]. Future studies aimed at elucidating the mechanisms underlying cellular internalization and trafficking of nanodroplets are certainly warranted. Nevertheless, based on the available data, it should be remarked that, the antimicrobial activity being equal, OLN formulations appear more suitable for topical use than OFNs.

However, OLN topical administration is not exempt from further issues. The skin, consisting of several layers including the stratum corneum, epidermis, and dermis, is the primary defense system of the body, and the stratum corneum, composed of corneocytes interspersed in a laminate of compressed keratin and intercorneocyte lipid lamellae, has a very low permeability to foreign molecules, thus being the main obstacle to transdermal drug delivery [6]. A number of methods have been proposed to overcome the natural barrier function of the skin, including skin patches, ionophoresis, use of chemical enhancers, and US-triggered sonophoresis [11]. Interestingly, antimicrobial properties have been reported for US, although its effectiveness strongly varies

depending on the targeted type of pathogen (fungi vs bacteria; cocci vs bacilli; Gram-positive vs Gram-negative etc.) [36].

Here, the ability of high frequency US to trigger chitosan OLN trespassing of the cutaneous layer was tested *in vitro*. Pig skin has been shown to have similar histological and physiological properties to human skin and has been suggested as a good model for human skin permeability. The histological characteristics of pig and human skin have been reported in literature to be comparable, with similarities existing for epidermal thickness and composition, pelage density, dermal structure, lipid content and general morphology [37]. Excited skin from the pig ear has become increasingly used in *in vitro* applications. The validity of the model has been established by comparing the permeability of simple marker molecules with the corresponding values across human skin [38-39]. The histology of porcine ear skin showed many similarities, as compared with human skin. The follicular structure also seemed to be very similar to that of humans. The porcine hairs and infundibula extend, similarly, deep into the dermis as in humans. In contrast to these results, the skin of other regions of the pig has shown more differences from human tissue. Therefore, porcine ear skin is the best suitable porcine *in vitro* model for human skin, e.g. in studies on percutaneous penetration [40]. In our experiments, US induced a significant OLN percentage (>15%) to cross pig skin membranes. Therefore, although further US administration did not affect OLN cytostatic properties against MRSA and *C. albicans*, sonication appears essential to promote chitosan OLN transdermal delivery during topical treatment.

Conclusion

The known benefits of nano-drug delivery, including size, stability, and encapsulation of a great range of therapeutics [41], combined with data showing that chitosan OLNs have both antimicrobial and tissue-oxygenating properties, suggest that the new nanodroplet platform has the potential to serve as a topical class of antimicrobial devices for adjuvant treatment of infected and hypoxic chronic wounds, as well as other cutaneous infections and inflammatory conditions. Even more so, OLNs offer the advantage of controlled release, being suitable for further functionalization, drug loading or encapsulation. Thus, they might provide future therapeutic opportunities to deliver multidrug regimens and combat resistant microbes as well as inflammatory disease states. Given the multi-faceted impact of OLNs, the present data inspire future *in vivo* studies to translate such a technology to clinical practice.

Future perspectives

Based on these promising results, antimicrobial OLNs are planned to be included in pharmaceutical formulations. Characterization of OLN-incorporating gels will be conducted via rheological behaviour of gels, mechanical strength and bioadhesion properties by texture profile analysis, and the nanosystems inside the gel formulations will be evaluated via submicron particle size measurement, differential scanning calorimetric analysis and diffusion studies through rat abdominal or pig ear skin. The formulations will be also tested for their safety profile in rodents. Thereafter, OLN effectiveness and feasibility will be assessed at the preclinical level through animal models of skin and soft tissue microbial infections, and further pharmacokinetic and pharmacodynamic studies will be carried out on the more promising formulations. Taken together, the results will pave the way for future clinical randomised trials.

Financial & competing interests disclosure

This work was supported by Compagnia di San Paolo (Ateneo-San Paolo 2011 ORTO11CE8R grant). A national patent request (TO2013A000707) for OLN manufacturing, characterization, and exploitation was deposited by the University of Torino on 2nd September 2013, and Caterina Guiot, Roberta Cavalli, and Mauro Prato were listed among the inventors. The authors have no other relevant affiliations or financial involvement with any organization or entity with a financial interest in or financial conflict with the subject matter or materials discussed in the manuscript. No writing assistance was utilized in the production of this manuscript.

EXECUTIVE SUMMARY

Characterization of chitosan-shelled nanodroplets

- Both chitosan-shelled OLNs and OFNs display spherical morphology.
- Both chitosan-shelled OLNs and OFNs display average diameters in the nanometer range (OLNs: ~700 nm; OFNs: ~300 nm).
- Both chitosan-shelled OLNs or OFNs display positively charged surface.

Antimicrobial effects of chitosan-shelled nanodroplets

- Both chitosan-shelled OLNs and OFNs are cytostatic against MRSA up to 4 h.
- Both chitosan-shelled OLNs and OFNs are cytostatic against *C. albicans* up to 24 h.
- Complementary US treatment does not alter antimicrobial properties of nanodroplets.

Cytotoxicity of chitosan-shelled nanodroplets on human skin cells

- Chitosan-shelled OLNs are not toxic on human keratinocytes.
- Chitosan-shelled OFNs slightly affect keratinocyte viability.
- Oxygen loading prevents chitosan nanodroplet toxicity to human keratinocytes.

US effects on chitosan-shelled nanodroplet transdermal delivery

- High frequency US effectively induces sonophoresis.
- High frequency US promotes OLN trespassing of pig skin layers.

Acknowledgements

Thanks are due to Adriano Troia for suggestions on nanodroplet manufacturing, to Marco Soster for help with SEM analysis, to Daniela Scalas for help with bacterial and fungal cultures, and to Francesca Silvagno for providing HaCaT cell line.

References

Papers of special note have been highlighted as:

• of interest; •• of considerable interest

1 Daeschlein G. Antimicrobial and antiseptic strategies in wound management. Int Wound J. 10 Suppl 1, 9-14 (2013).

2 Dietz I, Jerchel S, Szaszák M, Shima, K, Rupp J. When oxygen runs short: the microenvironment drives host-pathogen interactions. Microbes. Infect. 14, 311-6 (2012).

• comprehensive paper defining tissue hypoxia and discussing the abilities of infectious pathogens to adapt to low oxygen concentrations.

3 Gurusamy KS, Koti R, Toon CD, Wilson P, Davidson BR. Antibiotic therapy for the treatment of methicillin-resistant *Staphylococcus aureus* (MRSA) in non surgical wounds. Cochrane Database Syst. Rev. 11, CD010427 (2013).

4 Yang CH, He XS, Chen J, et al. Fungal infection in patients after liver transplantation in years 2003 to 2012. Ann. Transplant. 17, 59-63 (2012).

5 Percival SL, Hill KE, Malic S, Thomas DW, Williams DW. Antimicrobial tolerance and the significance of persister cells in recalcitrant chronic wound biofilms. Wound Repair. Regen. 19, 1-9 (2011).

6 Naik A, Kalia YN, Guy RH. Transdermal drug delivery: overcoming the skin's barrier function. Pharm. Sci. Technol. Today. 3, 318–26 (2000).

• comprehensive paper discussing the crucial role of US and what issues need to be faced to reach effective transdermal drug delivery.

7 Blecher K, Nasir A, Friedman A. The growing role of nanotechnology in combating infectious disease. Virulence. 2, 395-401 (2011).

8 Friedman AJ, Phan J, Schairer DO, et al. Antimicrobial and anti-inflammatory activity of chitosan-alginate nanoparticles: a targeted therapy for cutaneous pathogens. J. Invest. Dermatol. 133, 1231-9 (2013).

9 Li D, Diao J, Zhang J, Liu J. Fabrication of new chitosan-based composite sponge containing silver nanoparticles and its antibacterial properties for wound dressing. J. Nanosci. Nanotechnol. 11, 4733-8 (2011).

• this paper provides information on chitosan antimicrobial properties and its potential employment in nanopharmaceutical formulations for topical use.

10 Nath D, Banerjee P. Green nanotechnology - a new hope for medical biology. Environ. Toxicol. Pharmacol. 36, 997-1014 (2013).

11 Park D, Park H, Seo J, Lee S. Sonophoresis in transdermal drug delivery. Ultrasonics. 54, 56-65 (2014).

12 Cavalli R, Bisazza A, Rolfo A, et al. Ultrasound-mediated oxygen delivery from chitosan nanobubbles. Int. J. Pharm. 378, 215-7 (2009).

13 Cavalli R, Bisazza A, Giustetto P, et al. Preparation and characterization of dextran nanobubbles for oxygen delivery. Int. J. Pharm. 381:160-5 (2009).

14 Magnetto C, Prato M, Khadjavi A, et al. Ultrasound-activated decafluoropentane-cored and chitosan-shelled nanodroplets for oxygen delivery to hypoxic cutaneous tissues. R. S. C. Adv. 4, 38433-41 (2014).

•• this paper provides key information on chitosan-shelled OLN development, characterization, and effectiveness in releasing oxygen either *in vitro* or *in vivo*.

15 Prato M, Magnetto C, Jose J, et al. 2H,3H-decafluoropentane-based nanodroplets: new perspectives for oxygen delivery to hypoxic cutaneous tissues. Plos One. In press.

16 Banche G, Allizond V, Bracco P, et al. Interplay between surface properties of standard, vitamin E blended and oxidized UHMWPE for total joint arthroplasty and adhesion of *Staphylococcus aureus* and *Escherichia coli.* Bone Joint. J. 96, 497-501 (2014).

17 Boukamp P, Dzarlieva-Petrusevska RT, Breitkreuz D, Hornung J, Markham A, Fusenig NE. Normal keratinization in a spontaneously immortalized aneuploid human keratinocyte cell line. J. Cell. Biol. 106, 761-71 (1998).

18 Polimeni M, Valente E, Ulliers D, et al. Natural haemozoin induces expression and release of human monocyte tissue inhibitor of metalloproteinase-1. PLoS One. 8, e71468 (2013).

19 Skirtenko N, Tzanov T, Gedanken A, Rahimipour S. One-step preparation of multifunctional chitosan microspheres by a simple sonochemical method. Chemistry. 16, 562-7 (2010).

20 Schatz C, Viton C, Delair T, Pichot C, Domard A. Typical physicochemical behaviors of chitosan in aqueous solution. Biomacromolecules. 4, 641-8 (2003).

21 Shukla SK, Mishra AK, Arotiba OA, Mamba BB. Chitosan-based nanomaterials: a state-of-the-art review. Int. J. Biol. Macromol. 59, 46-58 (2013).

22 Zhang P, Cao M. Preparation of a novel organo-soluble chitosan grafted polycaprolactone copolymer for drug delivery. Int. J. Biol. Macromol. 65, 21-7 (2014).

23 Ma Y, Zhou T, Zhao C. Preparation of chitosan-nylon-6 blended membranes containing silver ions as antibacterial materials. Carbohydr. Res. 343, 230–7 (2008).

24 Goy RC, de Britto D, Assis OBG.A review of the antimicrobial activity of chitosan. Polímeros: Ciência e tecnologia. 19, 241-7 (2009).

25 Ueno H, Mori T, Fujinaga T. Topical formulations and wound healing applications of chitosan. Adv. Drug Deliv. Rev. 52, 105–15 (2001).

26 Chavez de Paz LE, Resin A, Howard KA, Sutherland DS, Wejse PL. Antimicrobial effect of chitosan nanoparticles on streptococcus mutans biofilms. Appl. Environ. Microbiol. 77, 3892–5 (2011).

27 Wu X, Landfester K, Musyanovych A, Guy RH. Disposition of charged nanoparticles after their topical application to the skin. Skin Pharmacol. Physiol. 23, 117-23 (2010).

28 Schutt EG, Klein DH, Mattrey RM, Riess JG. Injectable microbubbles as contrast agents for diagnostic ultrasound imaging: the key role of perfluorochemicals. Angew Chem. Int. Ed. Engl. 42, 3218-35 (2003).

29 Xia YP, Zhao Y, Tyrone JW, Chen A, Mustoe TA. Differential activation of migration by hypoxia in keratinocytes isolated from donors of increasing age: implication for chronic wounds in the elderly. J. Invest. Dermatol. 116, 50-6 (2001).

• this paper nicely shows how hypoxia differentially affects the production of tissue repair-related enzymes by human keratinocytes depending on donor's age.

30 Wiegand C, Winter D, Hipler UC. Molecular-weight-dependent toxic effects of chitosans on the human keratinocyte cell line HaCaT. Skin Pharmacol. Physiol. 23, 164-70 (2010).

31 Xie S, Tao Y, Pan Y, Qu W, Cheng G, Huang L, Chen D, Wang X, Liu Z, Yuan Z. Biodegradable nanoparticles for intracellular delivery of antimicrobial agents. J. Control. Release. 187, 101-17 (2014).

32 Treuel L, Jiang X, Nienhaus GU. New views on cellular uptake and trafficking of manufactured nanoparticles. J. R. Soc. Interface. 10, 20120939 (2013).

33 Johannes L, Lamaze C. Clathrin-dependent or not: is it still the question? Traffic. 3, 443-51 (2002).

34 Liu J, Shapiro JI. Endocytosis and signal transduction: basic science update. Biol. Res. Nurs. 5, 117-28 (2003).

35 Ivanov AI. Pharmacological inhibition of endocytic pathways: is it specific enough to be useful? Methods Mol. Biol. 440, 15-33 (2008).

36 Sango DM, Abela D, McElhatton A, Valdramidis VP. Assisted ultrasound applications for the production of safe foods. J. Appl. Microbiol. 116, 1067-83 (2014).

37 Dick IP, Scott RC. Pig ear skin as an in-vitro model for human skin permeability. J. Pharm. Pharmacol. 44, 640–5 (1992).

38 Herkenne C, Naik A, Kalia YN, Hadgraft J, Guy RH. Pig ear skin ex vivo as a model for in vivo dermatopharmacokinetic studies in man. Pharm. Res. 23, 1850-6 (2006).

39 Sekkat N(1), Kalia YN, Guy RH. Biophysical study of porcine ear skin in vitro and its comparison to human skin in vivo. J. Pharm. Sci. 91, 2376-81 (2002).

40 Jacobi U, Kaiser M, Toll R, Mangelsdorf S, Audring H, Otberg N, Sterry W, Lademann J. Porcine ear skin: an in vitro model for human skin. Skin. Res. Technol. 13, 19-24 (2007).

41 Schroeter A, Engelbrecht T, Neubert RHH, Goebel ASB. New Nanosized Technologies for Dermal and Transdermal Drug Delivery. A Review. J. Biomed. Nanotechnol. 6, 511–28 (2010).

Figure Legends

Figure 1. OLN and OFN morphology and size distribution. OLNs and OFNs were checked for morphology and size distribution by SEM and light scattering, respectively. Results are shown as representative images from twelve different preparations. Panel A. OLN image by SEM. Magnification: 5000X. Panel B. OLN size distribution. Panel C. OFN image by TEM. Magnification: 10000X. Panel D. OFN size distribution.

Figure 2. Antibacterial and antifungal activity of nanodroplets. Results are shown as means ± SEM from three independent experiments. Black columns: control populations; white columns: OFN-treated populations; jagged columns: OLN-treated populations. Panel A. Studies on MRSA growth. OLNs vs OFNs: p not significant (all times). OLNs/OFNs vs controls: * $p<0.02$ (3 and 4 h); p not significant (2 and 24 h). Panel B. Studies on *C. albicans* growth. OLNs vs OFNs: p not significant (all times). OLNs/OFNs vs controls: * $p<0.002$ and ** $p<0.001$ (2 h); * $p<0.001$ and ** $p<0.0001$ (3 h); * $p<0.0001$ (4 h); * $p<0.001$ and ** $p<0.0001$ (24 h).

Figure 3. Nanodroplet cytotoxicity and effects on human keratinocyte viability. Nanodroplet cytotoxicity on HaCaT cells was measured through LDH assay (panel A), and cell viability by MTT assay (panel B). Results are shown as means ± SEM from three independent experiments. Panel A. OFN-treated vs untreated cells: * $p<0.001$. OLN-treated vs untreated cells: p not significant. Panel B. OFN-treated vs untreated cells: * $p<0.001$. OLN-treated vs untreated cells: p not significant.

Figure 4. High frequency US-triggered OLN transdermal delivery: analysis by optical microscopy. To evaluate US ability to promote OLN trespassing through the skin, a home-made apparatus consisting of two sealed cylindrical chambers (donor and recipient, respectively) separated by a layer of pig ear skin was

employed. The donor chamber (filled with OLNs) was connected to an US-transducer (f = 2.5 MHz; P = 5 W), which was alternatively switched on and off at regular time intervals of 5 min for 135 min. Thereafter, the passage of OLNs from the donor to the recipient chamber was visualized by optical microscopy using a Leitz instrument. Results are shown as representative images from one out of three independent experiments. Magnification: 630X. Panel A: OLN-filled donor chamber before US treatment. Panel B: OLN-free recipient chamber before US treatment. Panel C: donor chamber after US treatment. Panel D: recipient chamber after US treatment.

TABLES

Table 1. Physico-chemical characterization of OLNs and OFNs. The nanodroplet formulations employed in the present study were characterized for average diameters, polydispersity index, and zeta potential by light scattering and for oxygen content through a chemical assay (see Materials and Methods). Results are shown as means ± SD from twelve preparations for each formulation.

Formulation	**Diameter (nm)**	**Polydispersity index**	**Zeta potential (mV)**	**Oxygen content (mg/ml)**
OLNs	727.70 ± 111.60	0.10	+ 35.89 ± 1.00	0.45 ± 0.01
OFNs	329.99 ± 131.70	0.12	+ 34.67 ± 1.00	-

Table 2. **Viscosity of chitosan solution and nanodroplet formulations before and after UV irradiation.** The viscosity (cP) of OLN and OFN suspensions as well as a solution of free chitosan was determined either before or after 20 minutes of UV sterilization at 25 °C by using a Ubbelohde capillary viscosimeter. The results are reported in the table.

	Chitosan solution	**OLNs**	**OFNs**
before UV	5.00 cP	4,62 cP	4,65 cP
after UV	5.00 cP	4,64 cP	4,66 cP

Table 3. High frequency US-triggered OLN transdermal delivery: measurement of fluorescent chitosan levels. Chitosan concentrations in both chambers of the home-made apparatus for transdermal delivery (see Figure 4), either before or after US treatment, are expressed as mg/ml. Results are shown as means ± SD from three independent experiments. All differences were significant, with $p<0.001$.

	before US	**after US**
donor chamber	1.13 ± 0.02 mg/ml	0.97 ± 0.06 mg/ml
recipient chamber	0 ± 0.00 mg/ml	0.18 ± 0.01 mg/ml

Fig. 1

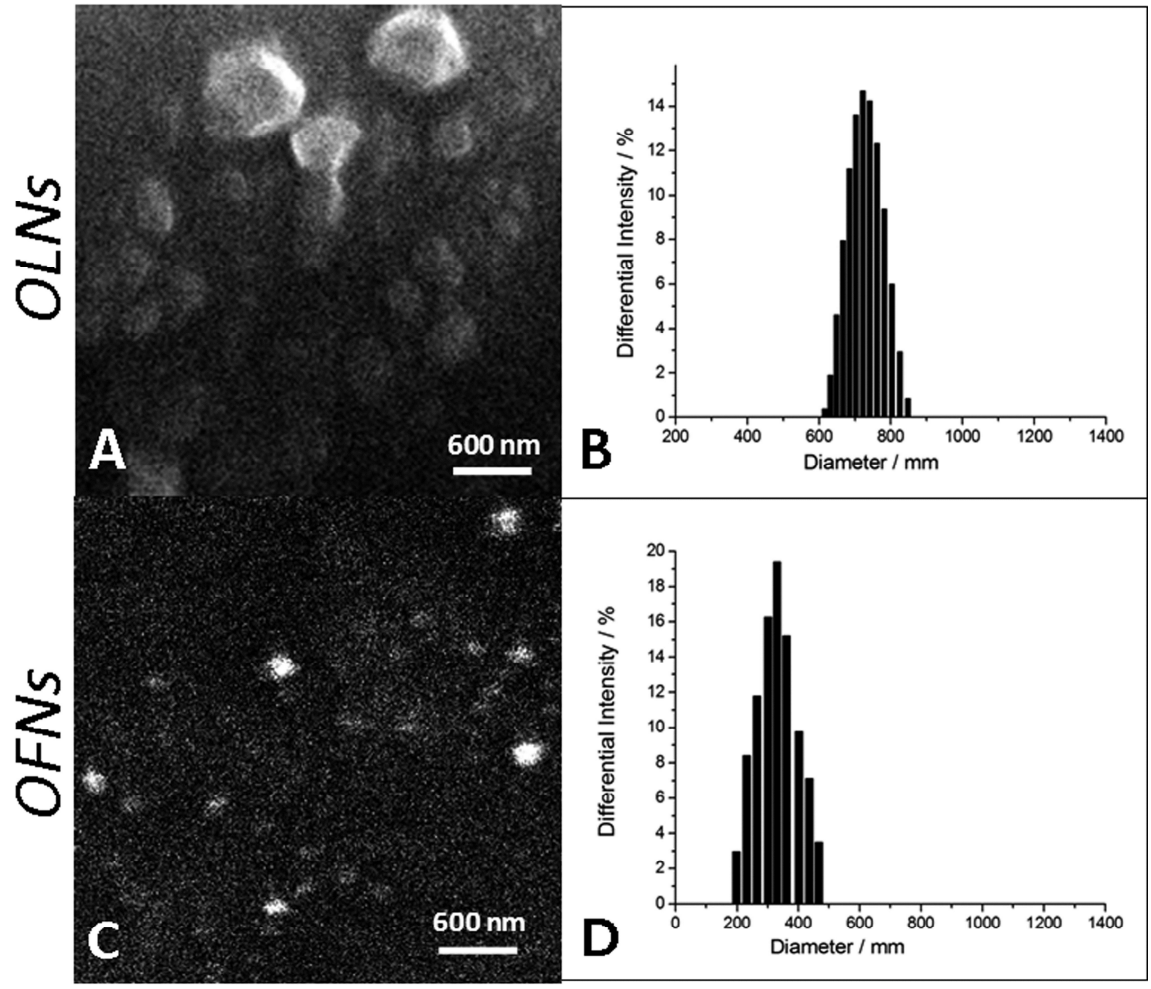
OLNs
A
600 nm
B
Differential Intensity / %
Diameter / mm
OFNs
C
600 nm
D
Differential Intensity / %
Diameter / mm

Fig. 2

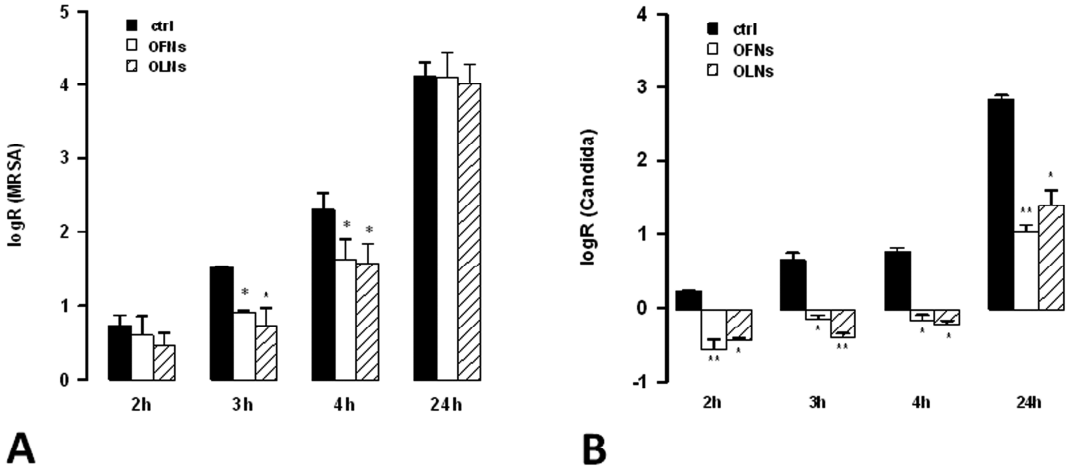
ctrl
OFNs
OLNs
logR (MRSA)
5
4
3
2
1
0
2h
3h
4h
24h
A
ctrl
OFNs
OLNs
logR (Candida)
4
3
2
1
0
-1
2h
3h
4h
24h
B

Fig. 3

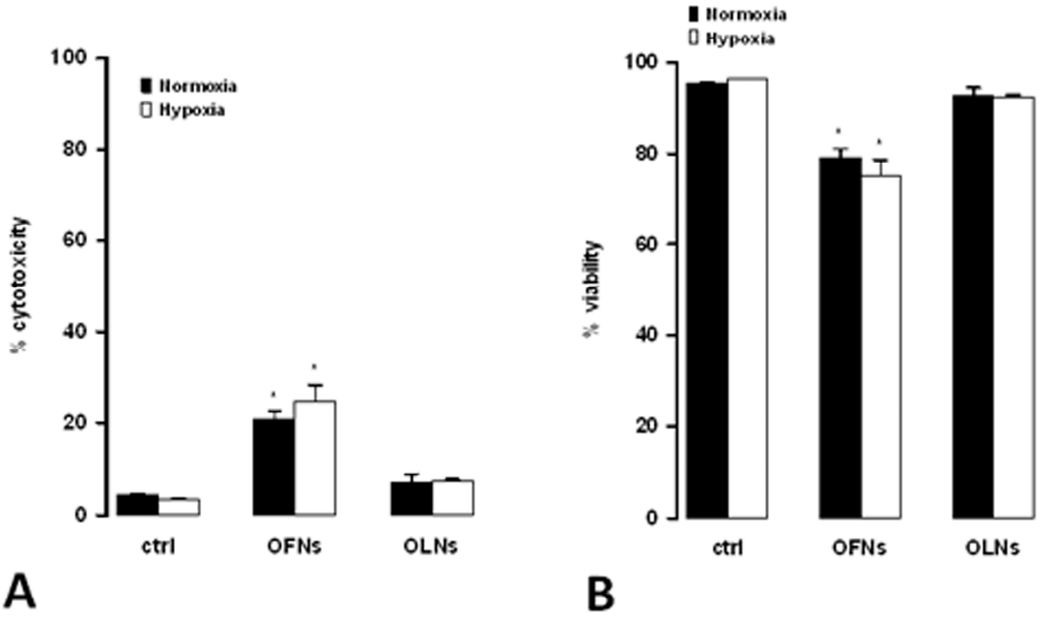
Normoxia
Hypoxia
% cytotoxicity
100
80
60
40
20
0
ctrl
OFNs
OLNs
A
Normoxia
Hypoxia
% viability
100
80
60
40
20
0
ctrl
OFNs
OLNs
B

Fig. 4

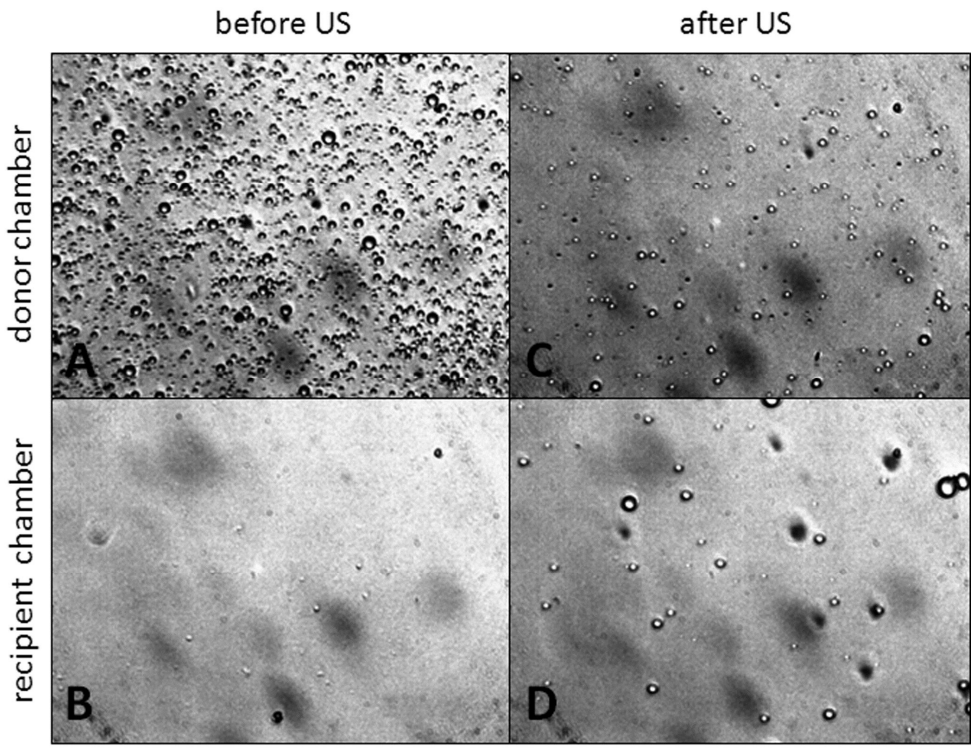
before US
after US
donor chamber
recipient chamber
A
B
C
D